

Measuring the Galactic Binary Fluxes with LISA: Metamorphoses and Disappearances of White Dwarf Binaries

Naoki Seto

Department of Physics, Kyoto University, Kyoto 606-8502, Japan

(Dated: January 12, 2022)

The space gravitational wave detector LISA is expected to detect $\sim 10^4$ of nearly monochromatic binaries, after ~ 10 yr operation. We propose to measure the inspiral/outspiral binary fluxes in the frequency space, by processing tiny frequency drifts of these numerous binaries. Rich astrophysical information is encoded in the frequency dependencies of the two fluxes, and we can read the long-term evolution of white dwarf binaries, resulting in metamorphoses or disappearances. This measurement will thus help us to deepen our understanding on the strongly interacting exotic objects. Using a simplified model for the frequency drift speeds, we discuss the primary aspects of the flux measurement, including the prospects with LISA.

Introduction.— Galactic ultra-compact binaries (orbital periods less than ~ 10 min) are secure and important observational targets for the space gravitational wave (GW) interferometer LISA [1, 2]. They are also promising systems for multi-messenger observations [3, 4]. By efficiently analyzing their data, we will be able to obtain fruitful information on strongly interacting exotic objects.

Most of these ultra-compact binaries would be detached white dwarf binaries (WDBs) and AM CVn-type systems, both emitting nearly monochromatic GWs [5–8]. The formers are at the inspiral phase ($\dot{f} > 0$, f : GW frequency), and eventually their less massive white dwarfs fill the Roche-lobes, initiating the mass transfer. In the basic picture, after this stage, the subsequent evolution bifurcates into two branches; survival or disappearance [6, 7, 9, 10]. If the mass transfer is stable, a WDB morphs into an AM CVn-type system, and its frequency turns into outspiral ($\dot{f} < 0$), keeping the Roche-lobe overflow. If the mass transfer is unstable, a WDB merges shortly, possibly accompanying an explosion event (e.g. type Ia supernova). But, at present, our understanding on the bifurcation (e.g. branching ratio) is quite limited, due to the lack of observational knowledge and the theoretically formidable physics on the strongly interacting compact objects [10, 11].

Even operating LISA for ten years, we are unlikely to observe a single WDB merger in the Galaxy, given its estimated merger rate $O(10^{-2})$ yr [7]. However, after such an operation period, LISA will measure small frequency drifts \dot{f} for $\sim 10^4$ of the ultra-compact binaries [3, 4].

In this letter, we propose to observationally determine the inspiral/outspiral binary fluxes, by using these swarm of binaries. We point out the importance of the frequency dependencies of the two fluxes, to statistically follow the destinies of the WDBs. Below, combining the basic picture for WDB evolution and a simplified model for the drift speed \dot{f} , we clarify the primary aspects of the flux measurement at $f \gtrsim 5$ mHz.

In fact, AM CVn systems are considered to be generated also from hybrid binaries of white dwarfs and non-

degenerate helium stars. Since they will emits GWs at most ~ 3 mHz [6, 7], we ignore this component below.

Binary fluxes.— In the basic picture, by tracing flows of inspiral binaries (see Fig. 1), we can easily understand their continuity equation in the frequency space, at the large number limit

$$\partial_t \rho_+(f, t) + \partial_f F_+(f, t) = \Sigma_{IJ}(f, t) - \Sigma_M(f, t) - \Sigma_T(f, t). \quad (1)$$

Here ρ_+ is the number density of inspiral binaries and F_+ is their flux. The three non-negative quantities Σ_{IJ} , Σ_M and Σ_T are the injection, merger and turnover rates (in units of $\text{Hz}^{-1}\text{s}^{-1}$). In the basic picture, the outspiral flux $F_- (\leq 0)$ is sourced by the turnover rate (see Fig. 1) and described by $\partial_t \rho_- + \partial_f F_- = \Sigma_T$, (ignoring potential disappearances after turnovers).

Our target band is $f \gtrsim 5$ mHz and almost all the WDBs there are expected to be generated at lower frequencies [7]. We thus put $\Sigma_{IJ} = 0$. Then, from Eq. (1), we have

$$F_+(f_1, t) - F_+(f_2, t) = \int_{f_1}^{f_2} [\Sigma_T(f, t) + \Sigma_M(f, t)] df + \frac{\partial}{\partial t} \int_{f_1}^{f_2} \rho_+(f, t) df \quad (2)$$

The last terms is the correction caused by the time variation of the inspiral flux F_+ . Considering the Galaxy-wide binary formation and the delay time distribution before chirping up to $f \sim 5$ mHz, the flux $F_+(f, t)$ (after suppressing the Poisson fluctuation) is expected to change slowly at the Hubble timescale $t_H \sim 10^{10}$ yr [3, 12]. Then, in Eq. (2), the last correction term will be $\sim t_d/t_H \sim 10^{-4}$ times smaller than the term $F_+(f_1, t)$. Here $t_d \sim 10^6$ yr is the characteristic transition time from f_1 to f_2 (above ~ 5 mHz). As we see later, the Poisson fluctuation of the fluxes (more than $\sqrt{10^{-4}} = 10^{-2}$) will completely mask the correction term of this level. We thus drop the time dependence of variables, and obtain

$$F_+(f_1) - F_+(f_2) = \int_{f_1}^{f_2} [\Sigma_T(f) + \Sigma_M(f)] df \quad (3)$$

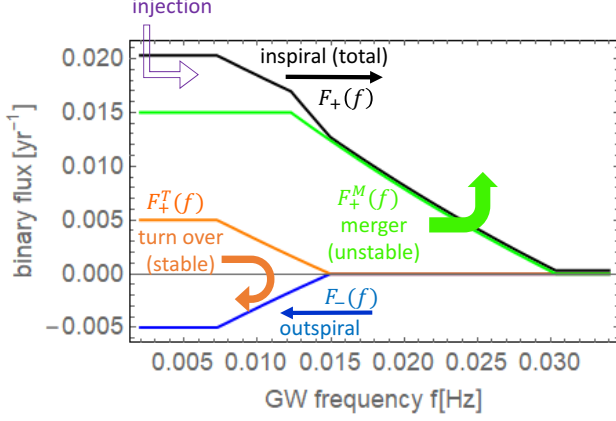


FIG. 1: The schematic picture for the inspiral/outspiral binary fluxes in the frequency space. The black curve shows the total inspiral flux $F_+(f) = F_+^M(f) + F_+^T(f)$ that is subdivided into the merger (green) and turnover (orange) components. The latter generates the outspiral flux $F_-(f) = -F_+^T(f)$ (blue). The information of the merger and turnover is clearly imprinted in the frequency dependencies of the two fluxes $F_{\pm}(f)$.

and similarly $F_-(f_1) - F_-(f_2) = -\int_{f_1}^{f_2} \Sigma_T(f) df$.

By observationally measuring the frequency dependencies of the two fluxes $F_{\pm}(f)$, we can separately estimate the two rates $\Sigma_M(f)$ and $\Sigma_T(f)$ at some frequency resolutions. This is the central part of the present proposal. Note that the conservation equations have been sometimes used theoretically, mainly for estimating the number densities of binaries (see e.g. [7, 13, 14]). But we use these equations in a completely different way.

Evolution of individual binaries.— Next, to discuss the flux measurement more concretely, we introduce a simplified model for the drift speed \dot{f} [3, 9] (see also [15–17]). This model would be a workable approximation to the steadily drifting binaries, except for the stages close to the merger or turnover frequencies. In fact, the binaries around the turn over $\dot{f} \sim 0$ would show somewhat complicated time evolution [18, 19]. But these binaries individually have small contributions ($\propto \dot{f}$) to the overall fluxes $F_{\pm}(f)$. We should also stress that, at actual observational measurement of the fluxes, we do not need detailed theoretical models for the drift speeds.

We first describe our simplified drift model for a circular inspiraling WDB ($\dot{f} > 0$). We denote its two initial masses by m_1 and m_2 with $m_1 \leq m_2$, and define the initial mass ratio $q \equiv m_1/m_2 \leq 1$.

Under the point particle approximation with the orbital separation a , the GW frequency f is given by $f = \pi^{-1}[G(m_1 + m_2)a^{-3}]^{1/2}$ and orbital angular momentum by $J = G^{1/2}a^{1/2}(m_1 + m_2)^{-1/2}m_1m_2$. Due to

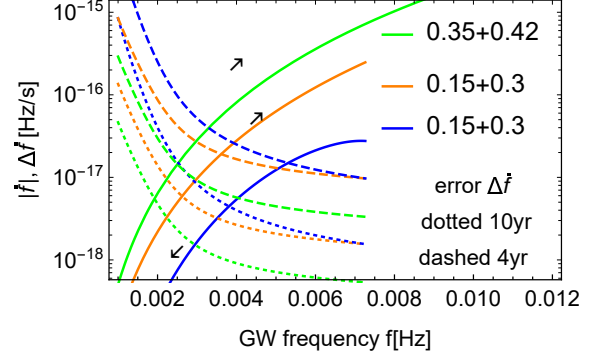


FIG. 2: The drift speeds $|\dot{f}|$ for the binaries with initial masses $0.35M_{\odot} + 0.46M_{\odot}$ (green) and $0.15M_{\odot} + 0.3M_{\odot}$ (orange: inspiral, blue: outspiral phases). The dotted and dashed curves show the estimations errors $\Delta\dot{f}$ for corresponding binaries at $d = 20\text{kpc}$ with the observational periods $T_o = 10\text{yr}$ and 4yr .

the angular momentum loss by GW emission, we have

$$\frac{\dot{f}}{3f} = -\frac{1}{2} \frac{\dot{a}}{a} = -\frac{J}{(J)_{\text{gw}}} = \frac{32G^{5/3}\pi^{8/3}\mathcal{M}^{5/3}f^{8/3}}{5c^5} \equiv t_{\text{gw}}^{-1} \quad (4)$$

with the chirp mass $\mathcal{M} \equiv (m_1m_2)^{3/5}(m_1 + m_2)^{-1/5}$.

We use the mass-radius relation $r(m)$ for completely degenerate helium in [20] originally given by P. Eggleton (see e.g. [21] for thermal effects). The Roche lobe radius of the less massive one is roughly given by $R_L \simeq 3^{-4/3}2a m_1^{1/3}(m_1 + m_2)^{-1/3}$ [9]. It shrinks, as the orbital separation a decreases. Eventually the WD fills the Roche lobe at the separation with $R_L = r(m_1)$. The GW frequency at this moment is given by

$$f_R(m_1) = \frac{2^{3/2}}{9\pi} \sqrt{\frac{Gm_1}{r(m_1)^3}} \quad (5)$$

as a function of the initial mass m_1 [22]. Now the less massive WD becomes a donor of the mass transfer to the more massive WD. If the initial mass ratio satisfies the following inequality ($\zeta(m) \equiv d \ln r(m)/d \ln m$)

$$q = \frac{m_1}{m_2} > \frac{3\zeta(m_1) + 5}{6}, \quad (6)$$

the mass transfer is unstable and two WDs merge [3, 9]. Here we assumed the conservative mass transfer and efficient angular momentum redistribution to the orbital component. The related physical parameters are not well understood at present [11, 15, 16], and our flux approach would provide us with useful information. For idealized cold Fermi gas at the non-relativistic limit, we have $\zeta = -1/3$ and $q > 2/3$ for Eq. (6).

In Fig. 2, with the green curve, we show the model prediction \dot{f} for WDB with initial masses $0.35M_{\odot} + 0.42M_{\odot}$

($q = 5/6$). This binary satisfies the unstable condition (6) and merges around $f_R(m_1) = 17.8\text{mHz}$ ($2.4 \times 10^6\text{yr}$ after passing 5mHz).

If the condition (6) does not hold, the mass transfer is stable and the binary becomes an AM CVn-type system, turning from inspiral ($\dot{f} > 0$) to outspiral ($\dot{f} < 0$) in the frequency space.

During the outspiral phase, the donor continuously fills the Roche lobe and its decreasing mass is given by the GW frequency as $m_{1e}(f) = f_R^{-1}(f)$ with the inverse relation of Eq. (5) [22]. For the accretor, we have $m_{2e}(f) = m_1 + m_2 - m_{1e}(f)$. Including the effects of the mass transfer, the frequency derivative of the outspiral phase is given by

$$\frac{\dot{f}}{f} = -\frac{3\dot{a}}{2a} = \frac{3}{2} \left(\zeta(m_{1e}) - \frac{1}{3} \right) \left(\frac{\zeta(m_{1e})}{2} + \frac{5}{6} - \frac{m_{1e}}{m_{2e}} \right) t_{\text{gw}}^{-1} \quad (7)$$

where the chirp mass in t_{gw} should be evaluated with the two evolved masses.

In Fig. 2, we show \dot{f} for a WDB with initial masses $0.15M_\odot + 0.3M_\odot$ ($q = 1/2$ and $\zeta(m_1) = -0.33$). In the basic picture, this binary initially moves on the orange curve up to $f_R(m_1) = 7.3\text{mHz}$. With stable mass transfer, it starts outspiral along the blue curve. Due to the effects of the chirp mass and the second parenthesis in Eq. (7), the outspiral rate is much smaller than the inspiral rate. It takes $1.1 \times 10^6\text{yr}$ for this binary to move from 5.0mHz up to 7.3mHz , and $5.9 \times 10^6\text{yr}$ to go back from 7.3mHz down to 5.0mHz .

In reality, a relatively diffuse envelope of the donor could be stripped at the late inspiral phase [18, 19]. But this would not change the concept of the flux approach (e.g. by using an appropriate relation $r(m)$ at the stage of interpreting the measured fluxes).

Flux model.— We now discuss the frequency dependence of the Galactic inspiral and outspiral fluxes. For the former, we put the total value

$$F_+(3\text{mHz}) = 0.02\text{yr}^{-1} \quad (8)$$

at 3mHz with no additional injection above this frequency [7]. This flux is divided into the merger and turn-over components F_+^M and F_+^T (see Fig. 1).

For the merger flux, we set $F_+^M(3\text{mHz}) = 0.015\text{yr}^{-1}$, following [7] ($\sim 10^3$ larger than double neutron stars [23]). For its mass distribution, we fix the initial ratio at $q_M = 5/6$ and assume a flat profile for m_1 in the range $0.25M_\odot \leq m_1 \leq 0.54M_\odot$. Here we set the massive end $0.54M_\odot$ so that the characteristic frequency $f_R(0.54M_\odot) = 30\text{mHz}$ is close to the highest WDB frequency predicted in [7]. The lower end was chosen somewhat arbitrarily with $f_R(0.25M_\odot) = 12\text{mHz}$. Actually, the green curve in Fig. 1 shows the flux $F_+^M(f)$ obtained for the present setting. The nearly straight-line structure at $12\text{--}30\text{mHz}$ is due to the approximately linear relation $f_R(m)$ in the relevant mass range.

For the turnover flux, we assume $F_+^T(3\text{mHz}) = 0.005\text{yr}^{-1}$ as a model parameter [6, 7]. For its mass distribution, we fix $q_T = 1/2$ with a flat profile for m_1 in the range $0.15M_\odot \leq m_1 \leq 0.3M_\odot$. As a precaution, we set the lower end to the very small value with $f_R(0.15M_\odot) = 7.3\text{mHz}$ which corresponds to the minimum turnover/merger frequency f_l in Fig. 1. This frequency f_l is important for the flux analysis and worth further study. We also have $f_R(0.13M_\odot) = 6.3\text{mHz}$ and $f_R(0.17M_\odot) = 8.2\text{mHz}$ for two different masses. The upper mass $0.3M_\odot$ was selected to match the highest frequency of the Galactic AM CVns predicted in [7] with $f_R(0.3M_\odot) = 15\text{mHz}$. In Fig. 1, the orange curve shows the resultant turnover flux $F_+^M(f)$. The outspiral flux (blue curve) is given by $F_-(f) = -F_+^T(f)$ in the simplified picture. We should comment that the magnitude of the turnover flux $F_+^T(3\text{mHz})$ is more uncertain than the merger flux $F_+^M(3\text{mHz})$. In a pessimistic model with an inefficient angular momentum redistribution [6, 7], the flux $F_+^T(3\text{mHz})$ could be two order of magnitude smaller than the value adopted above.

From the fluxes $F_\pm(f)$ and the drift speeds \dot{f} for the composing binaries, we can evaluate the number densities of binaries per unit frequency interval $\rho_\pm(f) = F_\pm(f)/\overline{\dot{f}_\pm(f)}$ with the number weighted mean drift speed $\overline{\dot{f}_\pm}$. In Fig. 3, we present our numerical results. In contrast to the fluxes in Fig. 1, the magnitudes of the orange and blue curves are not the same, reflecting the difference between the inspiral/outspiral speeds f as in Fig. 2. At $f < f_l = 7.3\text{mHz}$, we have the well-known form $\rho_+(f) \propto f^{-11/3}$ simply determined by Eq. (4) [7, 13]. Above 5mHz , the total numbers of the inspiral and outspiral binaries are estimated to be 6700 and 11800. If we decrease the mass ratios (q_M, q_T) by 10% from the original setting ($5/6, 1/2$), the larger components m_2 are increased by 10%. With this modification, the profiles $F_\pm(f)$ in Fig. 1 are unchanged, depending basically on the distribution of m_1 . But the total numbers of binaries above 5mHz shrink to 6200 and 10400 respectively for inspiral and outspiral binaries, because of higher chirp rates $|\dot{f}|$.

GW observation and flux measurement.— We now discuss how to measure the two binary fluxes $F_\pm(f)$ with LISA. Our basic procedure will be to firstly identify a large number of binaries by fitting their parameters including \dot{f} , and subsequently calculate the fluxes using the detected binaries.

The angular-averaged strain amplitude of a nearly monochromatic binary at the distance d is given by [2]

$$h = \frac{8(GM)^{5/3}\pi^{2/3}f^{2/3}}{5^{1/2}c^{8/3}d}. \quad (9)$$

Note that for an outspiral binary with $m_{1e} \ll m_{2e}$, we have $\mathcal{M}^{5/3} \sim m_{1e}m_{2e}^{2/3} \sim m_{1e}m_2^{2/3}$ and the amplitude depends weakly on the assumption on the mass conser-

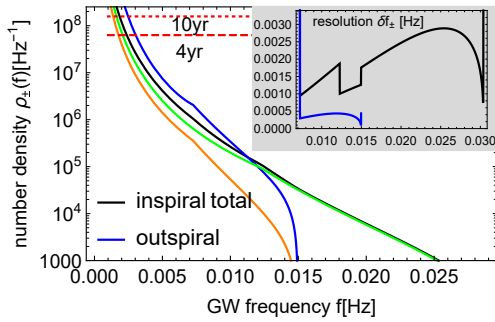


FIG. 3: The number densities of binaries per unit frequency. The black line is that for total inspiral binaries $\rho_+(f)$ composed by the merger (green) and turnover (orange) components. The blue curve is $\rho_-(f)$ for the outspiral binaries. The horizontal red lines show the critical densities for the source confusion. The inset shows the characteristic frequency resolutions δf_{\pm} in Eq. (14). The relative Poisson fluctuations are given by $[\rho_{\pm}(f)\delta f_{\pm}]^{-1/2}$.

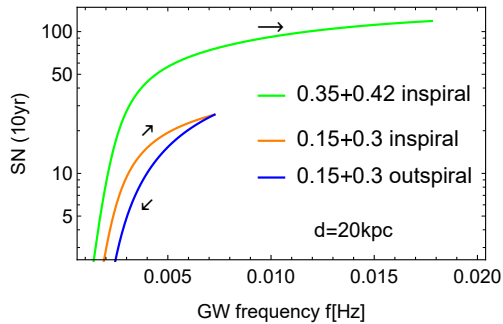


FIG. 4: The angular-averaged signal-to noise ratios for WDBs at $d = 20$ kpc and $T_o = 10$ yr. The green curve is for the initial masses $0.35M_{\odot} + 0.42M_{\odot}$, resulting in the merger. The WDB initially with $0.15M_{\odot} + 0.3M_{\odot}$ turns over at 7.2 mHz.

vation. The angular-averaged signal-to-noise ratio is estimated to be

$$SN = hT_o^{1/2}/S_n(f, T_o)^{1/2} \quad (10)$$

with the observational time T_o and the strain noise $S_n(f, T_o)$ composed by the instrumental and confusion noises. Here we included the T_o dependence of the confusion noise [2, 23].

In Fig. 4, we show the signal-to-noise ratios for binaries at $d = 20$ kpc and $T_o = 10$ yr. Almost all Galactic binaries have distances less than 20 kpc [3, 12, 13]. The blue curve (for the initial masses $0.15M_{\odot} + 0.3M_{\odot}$) can be regarded as the weakest signal emitter in the relevant frequencies regime (and smallest $|\dot{f}|$ except for those around the turnover). Since an edge-on binary has $\sqrt{5}/4 \sim 0.6$ times smaller amplitude than Eq. (10), we might miss some of outspiral binaries at $f \lesssim 5$ mHz with $SN \lesssim 10$.

For $T_o \gtrsim 2$ yr, the measurement error for the drift speed is estimated to be

$$\Delta \dot{f} = 4SN^{-1}T_o^{-2}, \quad (11)$$

and depends strongly on T_o [24]. In Fig. 2, with the dotted and dashed curves, we show the errors $\Delta \dot{f}$ for binaries identical to those in Fig. 4. For $T_o \sim 10$ yr, LISA is likely to have a resolution $\Delta \dot{f}/\dot{f} \lesssim 0.2$ at $f \gtrsim 5$ mHz, even for the smallest steady speed \dot{f} (blue curve).

Here we briefly comment on the potential signal overlapping. For each drifting binary, the number of fitting parameters is eight, and we need two frequency bins to determine them (using four complex numbers from two data channels) [25]. Therefore, the densities should be $\rho_+(f) + \rho_-(f) \lesssim T_o/2$ for resolving binaries. As shown in Fig. 3, for $T_o \gtrsim 4$ yr, the signal confusion would not be a fundamental problem at $f \gtrsim 5$ mHz (see also [12]).

Next we discuss how to estimate the inspiral flux $F_+(f)$ at a frequency f . We can make almost the same argument for the outspiral flux $F_+(f)$. Let us suppose that there are altogether $N_+^{\delta f}$ inspiral binaries in the frequency range $[f - \delta f/2, f + \delta f/2]$ with $\delta f \ll f$. With their label i , the inspiral flux can be estimated as

$$F_+^{\delta f}(f) = \sum_{i=1}^{N_+^{\delta f}} \frac{\dot{f}_i}{\delta f}. \quad (12)$$

As we mention earlier, the binaries around turnover $\dot{f} \sim 0$ individually have small contributions to this expression. We have the expectation values $\langle N_+^{\delta f} \rangle \simeq \rho_+(f)\delta f$ and $\langle F_+^{\delta f}(f) \rangle \simeq F_+(f) = \rho_+(f)\overline{\dot{f}_+}(f)$ with the mean inspiral speed $\overline{\dot{f}_+}(f)$. The latter $\langle F_+^{\delta f}(f) \rangle$ is independent of the width δf , but it has a statistical fluctuation $\Delta F_+^{\delta f}(f)$ in actual data reduction, due to the finiteness of the sample. More specifically, we can write down

$$\frac{\Delta F_+^{\delta f}(f)}{F_+(f)} \sim (N_+^{\delta f})^{-1/2} \left(1 + \frac{\sigma_{sc}}{\overline{\dot{f}_+}} + \frac{\sigma_{obs}}{\overline{\dot{f}_+}} \right). \quad (13)$$

The three terms in the last parenthesis originate from (i) the Poisson fluctuation of the sample number, (ii) the intrinsic scatter σ_{sc} of the speed \dot{f} and (iii) the typical magnitude σ_{obs} of the measurement error $\Delta \dot{f}$. For $f \gtrsim 5$ mHz and $T_o \sim 10$ yr, the third one would be negligible (see Fig. 2). Assuming $\sigma_{sc} \sim \overline{\dot{f}_+}$, we have $\Delta F_+^{\delta f}(f)/F_+(f) \sim (N_+^{\delta f})^{-1/2}$ corresponding to the Poisson fluctuation. For example, with our model parameters, we have the inspiral and outspiral binaries of $N_+ = 2050$ and $N_- = 3840$ in the range [5.5 mHz, 6.5 mHz]. We thus measure the fluxes $F_{\pm}(6$ mHz) with Poisson fluctuations less than $\sim 3\%$. Without injections, mergers and turnovers in [3 mHz, 6.5 mHz], we will have $F_{\pm}(3$ mHz) = $F_{\pm}(6$ mHz).

As discussed earlier around Eqs. (2) and (3), at $f > f_i$, we also want to finely resolve the frequency dependence of the flux $F_+^{\delta f}$ by taking a small width δf . But, at the same time, the statistical error should be suppressed.

We can take a balance by choosing the width as $\Delta F_+^{\delta f} \simeq |F_+(f + \delta f/2) - F_+(f - \delta f/2)|$. Similarly considering the outspirals flux, we have the approximate solutions as

$$\delta f_{\pm} = \rho_{\pm}^{-1/3} |F_{\pm}|^{2/3} |dF_{\pm}/df|^{-2/3}. \quad (14)$$

As shown in Fig. 3, in the range $dF_{\pm}/df \neq 0$, we have $\delta f_+ \sim 1\text{-}3\text{mHz}$ and $\delta f_- \sim 0.2\text{-}0.4\text{mHz}$. For deriving Eq. (14), we approximately put $F_+(f + \delta f/2) - F_+(f - \delta f/2) \sim \delta f \cdot dF_+/df$. In Fig. 3, this derivative introduces the sharp features, reflecting the discontinuities of $dF_{\pm}(f)/df$ as seen in Fig. 1.

For these solutions δf_{\pm} , we have the corresponding numbers of binaries $\rho_{\pm}(f)\delta f_{\pm} \sim 1000\text{-}100$ in the 7-15mHz range and smaller at higher frequencies. Therefore, the typical magnitude of the Poisson fluctuation is $\sim 100^{-1/2} \sim 0.1$.

Discussion.— In this letter, we proposed to measure the Galactic binary fluxes, by using $\sim 10^4$ of WDBs detected by LISA. By studying the frequency dependencies (closely related to initial mass m_1) of the fluxes at $f \geq f_l$, we can clearly follow how WDBs disappear or survive, affected by physical processes on strongly interacting exotic objects. To examine further details of the binary evolution beyond the basic picture, we could additionally use the distribution of the drift speeds \dot{f} .

While untouched so far, the fluxes at $f < f_l$ would be also useful. We can check the stationary of the fluxes and study potential binary injections and disruptions there. To make a complete Galactic sample at relatively low frequency regime (e.g. $f \lesssim 5\text{mHz}$), other space interferometers (e.g. Taiji [26] and TianQin [27]) could make important contributions, given the expected performance of LISA shown in Figs. 2 and 4. We can also employ Galactic structure models to correct the contributions of distant binaries that have too small rates $|\dot{f}|$ or even too small amplitudes h [4, 12].

This work is supported by JSPS Kakenhi Grant-in-Aid for Scientific Research (Nos. 17H06358 and 19K03870).

[1] P. Amaro-Seoane *et al.* [LISA], [arXiv:1702.00786 [astro-ph.IM]].

[2] T. Robson, N. J. Cornish and C. Liu, *Class. Quant. Grav.* **36**, no.10, 105011 (2019) doi:10.1088/1361-6382/ab1101 [arXiv:1803.01944 [astro-ph.HE]].

[3] G. Nelemans, L. R. Yungelson and S. F. Portegies Zwart, *Mon. Not. Roy. Astron. Soc.* **349**, 181 (2004) doi:10.1111/j.1365-2966.2004.07479.x [arXiv:astro-ph/0312193 [astro-ph]].

[4] V. Korol, E. M. Rossi and E. Barausse, *Mon. Not. Roy. Astron. Soc.* **483**, no.4, 5518-5533 (2019) doi:10.1093/mnras/sty3440 [arXiv:1806.03306 [astro-ph.GA]].

[5] D. Hils, P. L. Bender and R. F. Webbink, *Astrophys. J.* **360**, 75-94 (1990) doi:10.1086/169098

[6] G. Nelemans, S. F. Portegies Zwart, F. Verbunt and L. R. Yungelson, *Astron. Astrophys.* **368**, 939-949 (2001) doi:10.1051/0004-6361:20010049 [arXiv:astro-ph/0101123 [astro-ph]].

[7] S. Nisanke, M. Vallisneri, G. Nelemans and T. A. Prince, *Astrophys. J.* **758**, 131 (2012) doi:10.1088/0004-637X/758/2/131 [arXiv:1201.4613 [astro-ph.GA]].

[8] K. Kremer, K. Breivik, S. L. Larson and V. Kalogera, *Astrophys. J.* **846**, no.2, 95 (2017) doi:10.3847/1538-4357/aa8557 [arXiv:1707.01104 [astro-ph.HE]].

[9] B. Paczynski, *Acta Astron.* **17**, 287 (1967).

[10] J.-E. Solheim *Publ.Astron.Soc.Pac.* **122** 1133 (2010).

[11] T. R. Marsh, G. Nelemans and D. Steeghs, *Mon. Not. Roy. Astron. Soc.* **350**, 113 (2004) doi:10.1111/j.1365-2966.2004.07564.x [arXiv:astro-ph/0312577 [astro-ph]].

[12] A. Lamberts, S. Blunt, T. B. Littenberg, S. Garrison-Kimmel, T. Kupfer and R. E. Sanderson, *Mon. Not. Roy. Astron. Soc.* **490**, no.4, 5888-5903 (2019) doi:10.1093/mnras/stz2834 [arXiv:1907.00014 [astro-ph.HE]].

[13] N. Seto, *Mon. Not. Roy. Astron. Soc.* **333**, 469 (2002) doi:10.1046/j.1365-8711.2002.05432.x [arXiv:astro-ph/0202364 [astro-ph]].

[14] A. J. Farmer and E. S. Phinney, *Mon. Not. Roy. Astron. Soc.* **346**, 1197 (2003) doi:10.1111/j.1365-2966.2003.07176.x [arXiv:astro-ph/0304393 [astro-ph]].

[15] V. Gokhale, X. M. Peng and J. Frank, *Astrophys. J.* **655**, 1010-1024 (2007) doi:10.1086/510119 [arXiv:astro-ph/0610919 [astro-ph]].

[16] J. Fuller and D. Lai, *Mon. Not. Roy. Astron. Soc.* **444**, no.4, 3488-3500 (2014) doi:10.1093/mnras/stu1698 [arXiv:1406.2717 [astro-ph.SR]].

[17] L. O. McNeill, R. A. Mardling and B. Müller, *Mon. Not. Roy. Astron. Soc.* **491**, no.2, 3000-3012 (2020) doi:10.1093/mnras/stz3215 [arXiv:1901.09045 [astro-ph.HE]].

[18] D. L. Kaplan, L. Bildsten and J. D. R. Steinfadt, *Astrophys. J.* **758**, 64 (2012) doi:10.1088/0004-637X/758/1/64 [arXiv:1208.6320 [astro-ph.SR]].

[19] T. M. Tauris, *Phys. Rev. Lett.* **121**, no.13, 131105 (2018).

[20] F. Verbunt and S. Rappaport, *Astrophys. J.* **332**, 193-198 (1988).

[21] C. J. Deloye, R. E. Taam, C. Winisdoerffer and G. Chabrier, *Mon. Not. Roy. Astron. Soc.* **381**, 525 (2007) doi:10.1111/j.1365-2966.2007.12262.x [arXiv:0708.0220 [astro-ph]].

[22] K. Breivik, K. Kremer, M. Bueno, S. L. Larson, S. Coughlin and V. Kalogera, *Astrophys. J. Lett.* **854**, no.1, L1 (2018) doi:10.3847/2041-8213/aaa23 [arXiv:1710.08370 [astro-ph.SR]].

[23] N. Seto, *Mon. Not. Roy. Astron. Soc.* **489**, no.4, 4513-4519 (2019) doi:10.1093/mnras/stz2439 [arXiv:1909.01471 [astro-ph.HE]].

[24] R. Takahashi and N. Seto, *Astrophys. J.* **575**, 1030-1036 (2002) doi:10.1086/341483 [arXiv:astro-ph/0204487 [astro-ph]].

[25] J. Crowder and N. Cornish, *Phys. Rev. D* **75**, 043008 (2007) doi:10.1103/PhysRevD.75.043008 [arXiv:astro-ph/0611546 [astro-ph]].

[26] W. R. Hu and Y. L. Wu, *Natl. Sci. Rev.* **4**, 685 (2017).

[27] J. Luo *et al.*, *Class. Quant. Grav.* **33**, no.3, 035010 (2016) doi:10.1088/0264-9381/33/3/035010 [arXiv:1512.02076 [astro-ph.IM]].